ELSEVIER

Geoderma 91 (1999) 261–279

GEODERMA

Stable carbon isotope signatures preserved in authigenic gibbsite from a forested granitic–regolith: Panola Mt., Georgia, USA

Paul A. Schroeder *, Nathan D. Melear

Department of Geology, University of Georgia, 210 Field Street, Athens, GA 30602-2501, USA

Accepted 2 February 1999

Abstract

Six samples, selected from a weathering profile developed on a granite in the Panola Mountain Research Watershed in the Georgia Piedmont were studied for their stable carbon isotopic properties. The purpose was to understand the relationship between the stable carbon isotopic composition of the organic matter pool and the preservation of carbon in the authigenic soil minerals. The method for yielding carbon from authigenic phases is based on that of Yapp and Poths [$^{13}C/^{12}C$ ratios of the FE(III) carbonate component in natural goethites. In: Taylor, H.P., O'Neil, J.R., Kaplan, I.R. (Eds.), Stable Isotope Geochemistry: A Tribute to Samual Epstein, The Geochemical Society. Special Publication No. 3, 257–270.] and uses the following sample treatments: (1) Separation of the < 2 μm fraction; (2) Four 10-day oxidation cycles with 30% H_2O_2; (3) 12-h open-system vacuum dehydration at 110°C; (4) 1-h close-system oxidation with 0.3 bar oxygen at 200°C; (5) Timed step-wise open-system extractions at 230° to 240°C; and (6) A final 15-min closed-system combustion at 850°C with 0.2 bar oxygen. The evolved carbon dioxide, cryogenically collected during step 5, is operationally defined as hydroxide-bound carbon. X-ray diffractometry (XRD) and differential-scanning-calorimetry (DSC) indicate that the predominant phase transition at 230°C is the dehydroxylation of gibbsite. Gibbsite content of the bulk soil/saprolite ranges from 3 to 12% by weight. Acid Fe-extraction analysis as well as XRD, DSC and color show that goethite occurs at levels of $< 1\%$ by weight. C/H ratios measured during incremental extraction did not produce time-dependent trends. This 'non-stoichiometric' water is attributed to the dehydration and dehydroxylation of coexisting halloysite. The stable carbon isotopic release curves for samples at depth (> 28 cm) initially yield values from -15 to -17‰ (PDB) and then with each time step lighten to values from -18 to -22‰. Samples near the surface (< 16 cm) yield initial values from -14 to -16‰. With successive time steps they

* Corresponding author. Tel.: +1-706-542-2384; Fax: +1-706-542-2425; E-mail: schroe@gly.uga.edu

PII: S0016-7061(99)00013-0

initially become heavy (−13 to −11‰) and then become lighter with values from −16 to −17‰. The average stable carbon isotopic values for the six samples show a gradient trend from −21‰ at depth (236 cm) to −14‰ near the surface (6 cm). These results indicate that gibbsite offers a similar potential as the pedogenic minerals calcite and goethite to be a recorder of soil carbon systematics.

Keywords: carbon; Georgia; gibbsite; isotope; saprolite

1. Introduction

The concept of using carbon isotopes in paleosols as a proxy for estimating paleo-atmospheric PCO_2 throughout the Phanerozoic has been important to the validation of modeling efforts such as the GEOCARB model used by Berner (1994). The basis for using paleosol proxies has been well documented by Cerling (1984) and comes by virtue of the carbon isotopic trends seen in modern soil calcretes. Yapp and Poths (1990, 1993) have further proposed that carbon, structurally bound as a carbonate radical in pedogenic goethites, should similarly record global changes in atmospheric PCO_2. The underlying assumptions that provide the basis for the paleo-CO_2 barometer of Yapp and Poths (1990) appear very well-founded however, the isotopic systematics have not been extensively studied in the context of goethite-forming environments in modern soils. The purpose of this paper is to document the nature of stable carbon isotopes associated with authigenic soil/saprolite phases formed on a forested granite terrain in the Piedmont of Georgia.

2. Background

Evidence for a minor ferric carbonate-bearing component in goethite was first realized by Yapp and Poths (1986), who observed small CO_2 releases during incremental heating of paleosol goethites from 160° to 270°C. The concurrent release of CO_2 and hydrogen along with the transformation of goethite to hematite suggested that the CO_2 is contained in the goethite crystal structure. The carbonate component in goethite has since been supported by Yapp and Poths (1990) who observe the presence of infrared absorption bands at 1515 and 1345 cm^{-1} in goethites with high carbon contents. These bands are suggestive of a split in the normally doubly degenerate υ_3 vibrational modes of a CO_3^{2-} group (Farmer, 1974).

At the same time, Yapp and Poths realized there was a carbonate component in goethite, Cerling (1991), Cerling et al. (1989), Quade et al. (1989) were noting that the near surface CO_2 concentrations in modern soil gases systematically increase with depth while their $\delta^{13}C$ values decrease. This phenomenon has been explained by the upward diffusive mass transfer of CO_2 derived from

the bacterial oxidation of organic matter in the soil and exchange with the atmospheric reservoir of CO_2. Typical biogenic fluxes of CO_2 from temperate forest soils are on the order of 9.5×10^{-3} moles h^{-1} m^{-2} (Schlesinger, 1977). Because the rate of new mineral formation (10^{-10} moles h^{-1} m^{-2}) is small compared to the CO_2 respired (Cerling, 1984), it seems reasonable that the isotopic composition of the pedogenic minerals containing carbon will be controlled by the composition of the soil CO_2. Cerling (1984) has noted the importance of photosynthetic pathways to soil CO_2 composition (i.e., C_3 vs. C_4 plants) while Quade et al. (1989) have documented the importance of soil respiration rates. A consequence of this process is the incorporation of unique stable isotopic signatures into the soil carbonates that reflect information about the $\delta^{13}C$ of the surface plant biomass and soil respiration rates.

Building on the concepts developed by Cerling et al. (1989), Yapp and Poths (1992) proposed that goethite can provide information on both atmospheric $\delta^{13}C$ composition and PCO_2. The measured isotopic value ($\delta^{13}C_m$) in the goethite along with the mole fraction of $Fe(CO_3)OH$ in goethite (X_m) and estimates for the atmospheric and oxidized organic matter isotopic values, ($\delta^{13}C_A$ and $\delta^{13}C_O$, respectively) allow for the determination of the mole fraction in equilibrium with the CO_2 of the atmosphere (X_A). This is accomplished by a plot of $\delta^{13}C_m$ vs. $1/X_m$ which yields a line with a slope related to X_A. If an ideal solution exists between end-member goethite and the carbonate component, then the PCO_2 of the paleo-atmosphere can be determined.

Yapp and Poths (1994) note the key issue of CO_2 concentration in the soils generated by microbial respiration and the importance of factors such as soil productivity vs. diffusion out of the soil. These factors and the validity of the above relationship have not been extensively studied in the context of authigenic oxy-hydroxide and hydroxide mineral formation in modern soils such as those of the southeastern United States. Additionally, factors such as crystal-chemical variations in the authigenic phases and the coexistence of other carbon-bearing authigenic phases are also in need of contextual study.

3. Materials and methods

3.1. Study site and sample processing

High-resolution collection of a soil/saprolite/rock sequence was conducted at the well-studied the Panola Mountain Research Watershed (PMRW) operated by United States Geological Survey (USGS) located in the Georgia Piedmont of the southeastern United States (Huntington et al., 1993). Scientific investigations prior to the establishment of the PMRW first included several descriptions of the flora (Bostick, 1968, 1971; Ragsdale and Harwell, 1969; Carter, 1978). The site was also described in a regional geologic context by Holland (1954). Since the

establishment of the USGS program, other studies have involved community analysis of above-ground vegetation using previous and current survey information to estimate biomass increments (Cappellato and Carter, 1988) and hydrological flow on hillslopes (McDonnell et al., 1996).

One of the major appeals of using the PMRW is the fact that the bedrock is dominated by Panola Granite (granodiorite composition). It is Mississippian age and characterized as a very homogeneous, medium-grain, dark-gray, biotite–oligoclase–quartz–microcline granite with no discernible foliation (Atkins and Higgins, 1980). Sampling was conducted at a summit site in the PMRW where the weathering profile is believed to be wholly residual (i.e., not colluvial). Samples were collected from a 1 m^2 pit, at specified depth intervals (see Table 1). Each sampling was homogenized, sealed in a plastic bag and stored with dried ice. Upon return to the lab, splits were made for (1) freeze drying and whole rock stable carbon isotope analysis, (2) whole-rock X-ray diffraction mineralogical analysis and, (3) size separation to the < 2.0 μm (equivalent spherical diameter) 'fine' fraction.

One 10-g aliquot of the fine fraction was treated at 25°C with 500 ml of 30% H_2O_2. This treatment was repeated four times with each step lasting 10 days, with centrifugation and H_2O_2 renewal occurring between each step. The last step included elevating the temperature to 60°C for 1 h. The Panola granite is known to contain trace quantities of metasomatic calcite (White et al., 1997). Therefore, all samples were rinsed with a 5% HCl solution to remove any potential carbonate components.

A second aliquot of the fine fraction was further processed for clay mineral X-ray diffractometry (XRD) analysis and treatment to concentrate goethite and hematite. A 5 M NaOH treatment described by Kampf and Schwertmann (1982)

Table 1
Isotopic and chemical summary of < 2 μm fraction for samples from the PMRW ridge crest weathering profile

Sample	Depth (cm)	$\delta^{13}C$ (‰)[a]	C/H[b]	Endotherms by DSC (°C)[c]	Al-extract (wt.%)[d]	Fe-extract (wt.%)[d]
PP1-3	6	−13.4	0.0081	269, 477	7.75	5.02
PP1-5	16	−15.8	0.0155	274, 481	7.51	5.68
PP1-6	28	−18.3	0.0145	270, 475	7.74	6.01
PP1-7	50	−18.4	0.0115	275, 484	6.21	5.84
PP1-13	160	−20.9	0.0203	260, 489	5.19	6.65
PP1-15	236	−20.0	0.0110	254, 494	4.36	6.14

[a]This is the average $\delta^{13}C$ value of the carbon component in dehydroxylated phases (goethite and gibbsite) as determined from the 230°–240°C dehydration steps.

[b]C/H = twice the average ratio of moles of CO_2 to moles of H_2O extracted during the three timed steps before the final step.

[c]Differential scanning calorimetry, equilibrated at 150°C, N atmosphere, 10°/min.

[d]HCl extractable method described by Schroeder and Pruett (1996).

was used to remove gibbsite and kaolin group minerals. Concentrates were finally treated with 30% H_2O_2 for the removal of labile organic matter. Approximately 500 mg of concentrate was added to 50 ml of H_2O_2 and then stirred on a shaker table at 25°C for 10 days. The mixture was then centrifuged at high speed and the supernatant was decanted. This last series of peroxide steps was repeated two more times by refreshing the 30% H_2O_2, re-suspending the concentrate and stirring for a minimum period of 10 days. Yapp (1991) has shown that this method can be used to purify well-crystalline goethite for $\delta^{18}O$ analysis without isotopic exchange.

3.2. CO_2 and H_2O extraction and mass spectrometry

Dehydration and decarbonation experiments were performed on a dedicated micro-volume extraction line built at the University of Georgia Geology Stable Isotope Laboratory. The extraction procedure is a modified version of the procedure described by Yapp and Poths (1991). Aliquots (1 g) of freeze-dried fine fraction were weighed into quartz tubes prepackaged with glass wool. For each extraction, a sample was placed under open vacuum conditions at 110°C overnight to allow for outgassing. Furnace temperatures were regulated by an Omega® programmable temperature controller, thus allowing for precise (± 2°C) ramping and maintaining of temperatures. A closed system oxidation step was performed to help remove additional organic carbon not released by peroxide treatments. This was accomplished by introducing approximately 0.5 bars of reagent grade tank oxygen into the sample-bearing portion of the extraction line. The temperature was ramped from 110° to 200°C. Oxygen was introduced and 200°C was maintained for a period of 1 h. During this time, evolved CO_2 and H_2O were vented under closed conditions. The temperature was then ramped to 230°C over a period of 15 min, at which time the system was left under open vacuum conditions. Once the furnace reached 230°C, CO_2 and H_2O were trapped with a liquid nitrogen (LN_2) cooled double-loop trap.

Step-wise extractions ranging from 30 to 120 min were conducted from 230° to 240°C, under open system conditions. Evolved CO_2 and H_2O were cryogenically trapped with the LN_2. At the end of each time period, the trapped gases were isolated from the sample and processed for separation and yield measurement of CO_2 and H_2O, respectively. H_2O was kept in the frozen state by replacing the trap with an ethyl alcohol and dry ice slush. CO_2 evolved by this heating was trapped in a cold finger with LN_2 and subsequently measured using a Hg micro-manometer, specially built to measure gas volumes in the range of 0.2–18.0 μmoles $\pm$ 0.1 μmoles. After the CO_2 yield measurement, CO_2 was then LN_2-trapped back into a stop-cock vessel for transfer to the mass spectrometer. Evolved H_2O was transferred to a stop-cock vessel, by removing the slush from the trap and re-freezing with LN_2 on the vessel. Each H_2O stop-cock vessel was previously filled with 200 mg of reagent-grade Sn. H_2O was

converted to H_2 by reaction with the Sn at 470°C in a furnace for 30 min. H_2 yields were subsequently measured using a Baratron® previously calibrated using known volumes of H_2 gas yielded from known masses of H_2O. H_2 yields were measured with a precision of ± 3 μmoles.

Unlike the method of Yapp and Poths (1991), which removes the mineral sample from the furnace during the processing of CO_2 and H_2O yield measurements, samples were allowed to continuously evolve gases under an open system vacuum. This was made possible through the development of a parallel system of extraction lines equipped with a duplicate set of trap, stop-cock vessel ports, cold finger, micro-manometer and vacuum gauges. A valved bifurcation in the line allowed the operator to toggle back and forth, extracting on one side, while processing on the other side, thus saving considerable time.

Carbon isotope ratios were measured on a Finnigan MAT 252 isotope ratio mass spectrometer housed at the University of Georgia Geology Isotope Laboratory. Results are reported using the usual $\delta^{13}C$ notation and the standard is PDB (Craig, 1957). Analytical error of $\delta^{13}C$ measurement with 0.5 μmole of the same gas sample is about ± 0.5‰.

Prior to the sample extractions, 'blanks' comprised of a poorly ordered Australian kaolinite (Schroeder et al., 1998) were subject to the described step-wise procedure. One sample was H_2O_2 treated and the other untreated. The untreated blank yielded small quantities of CO_2 and H_2O (1.3 μmole g^{-1} and 928 μmoles g^{-1}, respectively) and an average $\delta^{13}C$ of -22.7‰. The carbon yield and isotopic values are typical for kerogen found in clay-rich rocks (Tissot and Welte, 1978). The treated blank yielded slightly smaller quantities of CO_2 (1.0 μmole g^{-1}), suggesting that most of the organic matter in the blank was refractory. The blank experiments do however, indicate that even a poorly-ordered kaolinite, does not contribute significant quantities of CO_2 during the step-wise extraction.

Precision for the step-wise extraction of CO_2 and H_2O at 230° to 240°C was examined by a triplicate analysis of sample PP1-5. The average standard deviation for each of the five step intervals was 2.0‰. Yields of CO_2 and H_2O values during the first extraction step at 230°C typically resulted in wide-ranging C/H values. Subsequent steps produced C/H values that ranged from 0.0040 to 0.0100 with standard deviations of 0.0008 and 0.0044, respectively. The average C/H value for all PP1-5 runs, excluding the first step and last step was 0.0081.

3.3. Ancillary analytical methods

Aliquots of all samples were submitted to differential scanning calorimetry (DSC) and X-ray powder diffraction analysis. Selected samples were additionally examined using high-resolution DSC and infrared spectroscopy. Samples prepared for IR analysis using standard pressed KBr pellets mixed at proportions of 0.5 mg of sample with 150 mg of KBr powder. Details of these ancillary

XRD and DSC analytical procedures are fully described by Melear (1998) who examined the crystal-chemistry of the secondary phases within the same sample suite from the PMRW.

Total Fe content of the fine fraction material was also measured to estimate potential total goethite. Each sample was extracted with HCl according the method of Schroeder and Pruett (1996). Extractable Fe and Al contents were measured using the solution extract. Fe was measured using atomic absorption and Al with a Perkin–Elmer induction-coupled plasma mass spectrometer (ICP-MS), both at the University of Georgia's Department of Crop and Soil Science.

4. Results

4.1. Fine fraction mineralogy

Mineralogical analysis of fine fraction using XRD, DSC and IR methods shows that sample materials are composed of kaolin group minerals (kaolinite and halloysite), gibbsite. hydroxy-interlayer-vermiculite (HIV), goethite, hematite and quartz. Table 1 contains a summary of isotopic, mineralogical and chemical data collected for each sample. The fine fraction mineralogy is clearly dominated by the kaolin group minerals. Although kaolinite and halloysite were not explicitly quantified, the low angle asymmetry of the basal (001) reflection seen in the XRD data indicate that halloysite coexists with kaolinite. This is supported by the presence of tubular clay morphology seen in electron microscopy investigations of Ultisols in the southeastern U.S. Piedmont (Nixon, 1981; Dixon, 1989; Melear, 1990). The presence of halloysite and HIV is important because interlayer water is likely a factor in the production of non-stoichiometric hydrogen measured during the timed-step extractions.

Gibbsite is the second most dominant phase in the fine fraction assemblage. Fig. 1 shows the X-ray diffraction pattern of the sample PP1-5 at various stages of the procedure. Most notable is the disappearance of the gibbsite reflections after the last heating step at 240°C. DSC analysis of the same sample PP1-5 (Fig. 2) corroborate the fact that the dehydroxylation of gibbsite is the most volumetrically significant phase transformation occurring at 230° to 240°C.

The presence of goethite and hematite is confirmed by XRD (Melear and Schroeder, 1998) and IR analysis of the selectively NaOH dissolved samples. The aggressive chemical treatment makes attempts at quantifying the relative amounts of goethite vs. hematite in the extracted sample somewhat dubious. Estimates of goethite and hematite contents however can be made from an analysis of the average fine fraction total Fe content ($\sim$ 8.5% by weight Fe_2O_3) and light brown color (5 YR 5/6). Using the calibration of Munsell coloration vs. iron content of Hurst (1977), the fine fraction material approximates a

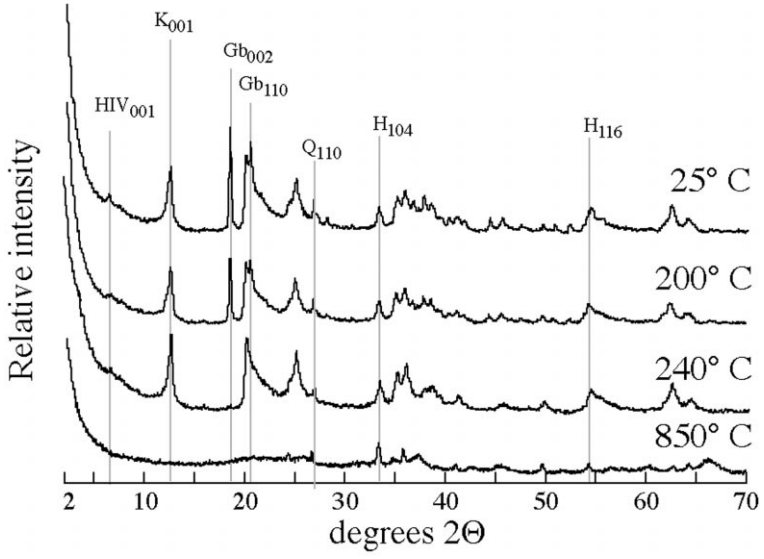

Fig. 1. X-ray diffractograms for the randomly-oriented < 2 μm fraction of sample PP1-5 before and after temperature treatments. The faint vertical lines mark the positions of various reflections for the phases, HIV, kaolin group minerals (K), gibbsite (Gb), quartz (Q) and hematite (H), respectively. Subscripts refer to reflection indices. Abscissa values are in °2Θ, using CuKα radiation.

goethite to hematite ratio of 1:5. This is indirectly supported by the relative intensities of the major XRD reflections for hematite seen in Fig. 1. XRD reflections for goethite are virtually unseen, which in part may be due to small coherent scattering domains (Hurst et al., 1997).

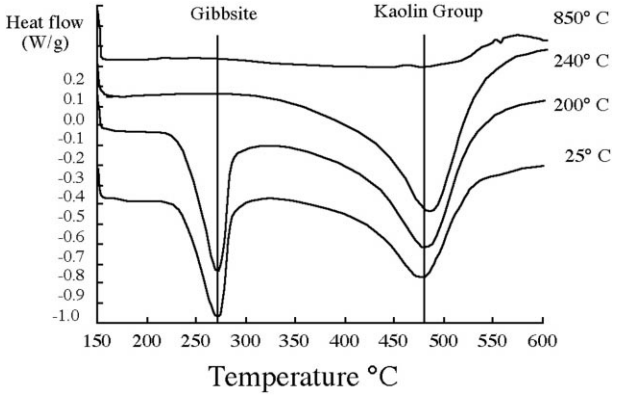

Fig. 2. Differential scanning calorimetry spectra for the < 2 μm fraction of sample PP1-5 before and after temperature treatments. Samples were equilibrated at 150°C and temperature ramped at 10° min^{-1} in a N atmosphere to 600°C. Spectra are presented at the same scale, but are vertically offset in increments of ± 0.2 W g^{-1} relative to the 200°C spectrum.

Using the above goethite to hematite proportion of 1:5, implies that goethite comprises no more than 1% by weight of the total fine fraction. This estimate is important because it indicates that if the observable upper limit for the mole fraction of carbon bound in goethite (X_m) is 0.018 (Yapp, 1996), then the probable upper limit on total CO_2 liberated from fine fraction material during the timed-step extractions is about 3 μmole g^{-1}. Actual CO_2 yields from time-step extractions ranged from 19 to 42 μmoles g^{-1}.

4.2. $\delta^{13}C$ observations

Bulk total carbon and $\delta^{13}C$ values for the soil/saprolite samples are presented in Table 2. The total carbon values, that range from 3.6% near the surface to 0.01% in the saprolite, are typical for a forested weathering profile in the temperate climate of the SE U.S. Piedmont (Singh and Gupta, 1977). The source of carbon input is clearly dominated by coniferous and deciduous leaf and wood litter accumulation. Plant root biomass and carbon metabolized by bacteria are also likely contributors to the soil carbon pool. It is assumed that carbon sequestered into authigenic minerals is volumetrically small relative to the coexisting organic matter. Therefore, the bulk $\delta^{13}C$ measurements reflect the soil organic matter values. The shallowest, carbon-rich litter layer has an isotopic value of −23.9‰. This is close to the −29.8 to −24.3 range reported by Balesdent et al. (1993) for leaves and soil organic matter in a temperate forest. The isotopic trend with depth presented in Table 2 is also consistent with Balesdent et al. (1993) observations, where $\delta^{13}C$ values increase (become heavier) directly below the litter horizon, with enrichments on the order of several parts ‰. Respiration rates are the greatest directly below the litter horizon (Singh and Gupta, 1977) and therefore, it is reasonable to assume that

Table 2
Whole soil/saprolite isotopic and mineralogical data for PMRW ridge crest weathering profile

Sample	Depth (cm)	Gibbsite (wt.%)[a]	$\delta^{13}C$ (‰)[b]	Carbon (wt.%)[c]
PP1-2	2	1.0	−23.9	3.64
PP1-3	6	9.2	−18.9	0.42
PP1-4	10	11.9	−21.5	0.39
PP1-5	16	12.1	−19.0	0.35
PP1-6	28	11.9	−23.5	0.29
PP1-7	50	11.6	–	0.20
PP1-9	80	7.5	–	0.12
PP1-12	140	10.5	−24.9	0.04
PP1-13	160	5.3	−24.5	0.03
PP1-15	236	2.2	–	0.01

[a]Determined by DSC calibrated to end-member gibbsite.
[b]Relative to PDB standard.
[c]Based on total CO_2 yield from 1000°C combustion with O_2.

the slight enrichments are a fractionation effect due to preferential bacterial consumption of isotopically lighter carbon. Interestingly, the $\delta^{13}C$ values asymptotically converge back to the leaf and woody material input value of about −25‰. Total carbon values are small at depth and likely represent translocated colloidal organic matter adsorbed on mineral surfaces, remains of bacterial cell growth and inorganic forms of carbonate sequestered by authigenic minerals.

Fig. 3 is designed to sequentially show the procedural history for each fine fraction sample. The stable carbon isotope release curves for samples at depth (> 28 cm) initially yield values from −16 to −18‰ and then with each time step lighten to values from −18 to −22‰. Samples near the surface (< 16 cm) yield initial values from −14 to −16‰. With successive time steps, they initially become heavy (−13 to −11‰) and then become lighter with values from −16 to −17‰. The final extraction at 850°C yields more tightly clustered values around −21 to −22‰. The CO_2 evolved during this last step is indubitably kerogen-like refractory organic matter, with isotopic values characteristic of terrestrially derived kerogen (Tissot and Welte, 1978).

C/H ratios measured during incremental extraction did not produce time-dependent trends or depth dependent trends. This variation is attributed to 'non-stoichiometric' hydrogen (water and/or surface structural OH, as noted by Yapp and Poths, 1993) that, in the case of our study, is most likely associated with halloysite and poorly ordered forms of Fe and Al hydroxides. Table 1 lists the

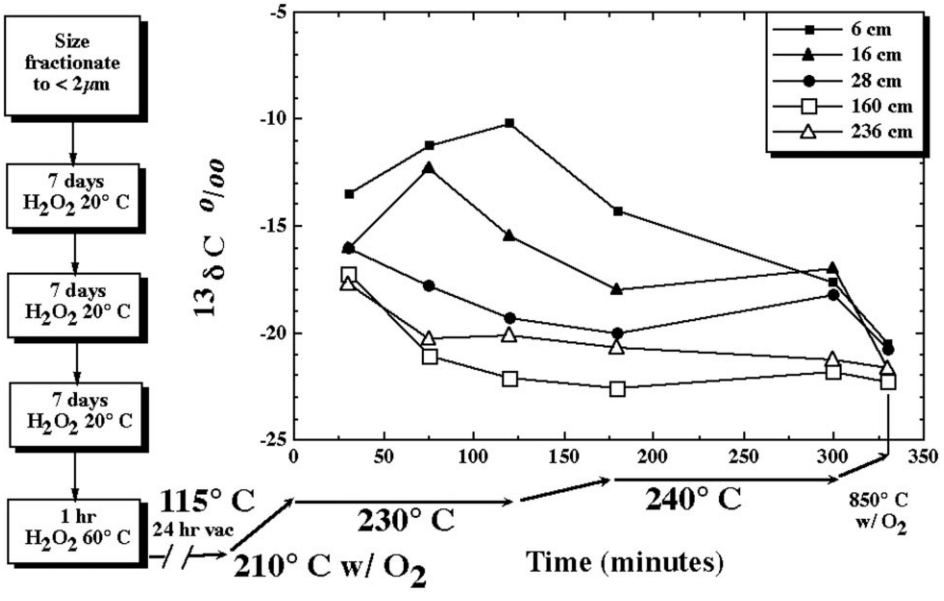

Fig. 3. Sample processing flow chart and incremental $\delta^{13}C$ values measured during the timed-step extractions. Steps prior to heated CO_2 extraction and subsequent isotopic measurement are designed to minimize CO_2 contribution from the oxidation of organic matter.

average C/H values for each of the samples, which vary from 0.013 to 0.030. There is no depth dependent trend, however, the range of values is notably similar to those observed from goethite found in modern soils (Hsieh and Yapp, 1999).

5. Discussion

Mineralogical analysis demonstrates that gibbsite dehydroxylation is the principle phase transformation taking place during the timed-step extractions of the fine fraction material from the PMRW weathering profile. During each extraction run, significant quantities (19–40 μmoles) of CO_2 are produced during the breakdown of gibbsite. The implications of these results is that gibbsite has the potential to record the soil carbon isotopic signature and can be used in a fashion similar to goethite as proposed by Yapp and Poths (1992).

The exact mechanism for the sequestering of carbon by gibbsite can only speculated upon at this point in time, since the yielding of CO_2 has only been recognized in this study. Fig. 4 shows the crystal structure of gibbsite. It is comprised of the fundamental units of two planes of close-packed OH^- with

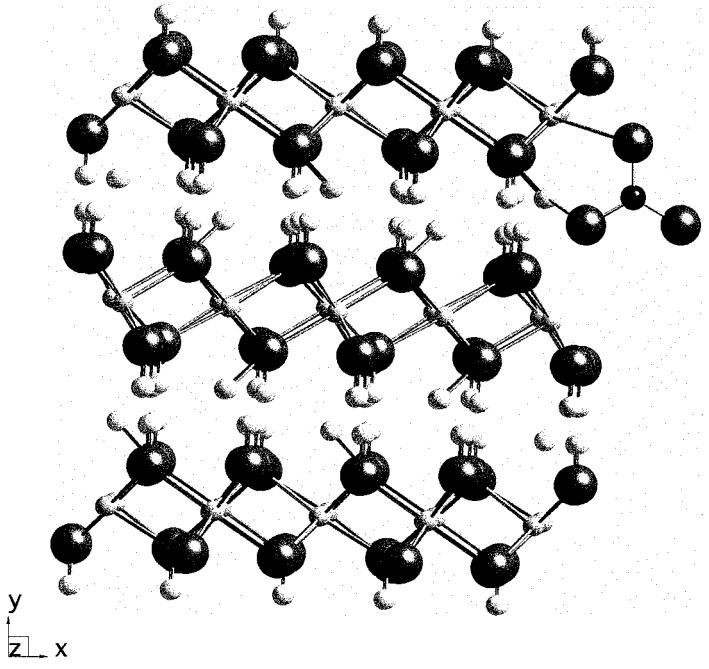

Fig. 4. Idealized crystal structure of gibbsite after Megaw (1934) viewed in the [010] direction. O and Al positions are shown as octahedrally coordinated atoms. Hydroxyl groups (i.e., protons) occupy the inter-octahedral layer region. The trigonal carbonate group bonded on the right edge of the structure depicts one possible carbon sequestering mechanism.

Al^{3+} sandwiched between them (Megaw, 1934). The gibbsite polymorph is arranged such that OH^- groups are stacked directly upon each via hydrogen bonding. Edges of the gibbsite structure have been shown to hold ligands to compensate for charge imbalances resulting from defects within the gibbsite structure (Hsu, 1989). Violante et al. (1993) have long noted the importance of organic ligands in controlling the precipitation kinetics of gibbsite under soil forming conditions. If organic ligands appear to facilitate gibbsite crystal growth, then perhaps small organic ligands dissolved in pore waters can be incorporated into the mineral structure during crystal growth. The defect-free gibbsite structure does not contain goethite-like *c*-axis parallel galleys that are proposed to house carbonate radicals (Yapp and Poths, 1990). Knowing whether the carbon yielded during the thermal breakdown of gibbsite is associated with a reservoir of dissolved organic ligands or with the dissolved inorganic carbon reservoir (i.e., equilibrated with soil gas CO_2) has implications for isotopic fractionation effects.

Fig. 5 shows a plot of the average (dots) and range (bars) of $\delta^{13}C$ values recorded for each sample vs. the sampling depth. Overlain from left to right are vertical lines that represent, (a) the average $\delta^{13}C$ composition of the input organic matter, (b) the 4.4‰ shift in $\delta^{13}C$ composition that would be expected in soil derived CO_2, and (3) the average $\delta^{13}C$ composition of a pre-industrial atmosphere. The observation that the $\delta^{13}C$ values of near-surface gibbsite-generated CO_2 are significantly heavier than both the gibbsite $\delta^{13}C$ values at depth and the $\delta^{13}C$ organic matter, suggests that the depth gradient reflects mixing between reservoirs. The relatively enriched ^{13}C-rich source is the atmospheric CO_2 reservoir which has an approximate interglacial pre-industrial $\delta^{13}C$ composition of -6‰. The coincidence of the CO_2 soil gas $\delta^{13}C$ composition and the $\delta^{13}C$ of deep samples suggests that the gibbsite-sequestered carbon is in isotopic equilibrium with the soil CO_2.

The exact mechanism for the apparent recording of soil $\delta^{13}C$ values with an apparent fractionation factor between mineral and CO_2 gas of ~ 1.000 in this soil is not clear at this time. The effect of carbon contributed by the contemporaneous dehydroxylation of goethite seems to be minimal. As mentioned in the results section above, the maximum goethite-CO_2 potentially liberated from 1 g of fine fraction material during the timed-step extractions is about 3 μmoles. Yields of CO_2 from this study ranged from 19 to 42 μmole g^{-1}. The range of $\delta^{13}C$ values recorded from natural goethites dehydroxylation is -21 to 3‰ (Yapp and Poths, 1993). It is therefore possible that the $\delta^{13}C$ values recorded in our study are biased by a goethite component. The effect however, would be indistinguishable if the goethite component was isotopically light (~ -20‰) or small if the goethite component was isotopically heavy (~ 3‰).

Regarding the nature of carbon sequestration by the gibbsite structure, Yapp (1987) has proposed that carbon sequestered into goethite resides as a solid-solution ($Fe(CO_3,O)OH$) with a distorted carbonate radical located in the *c*-axis

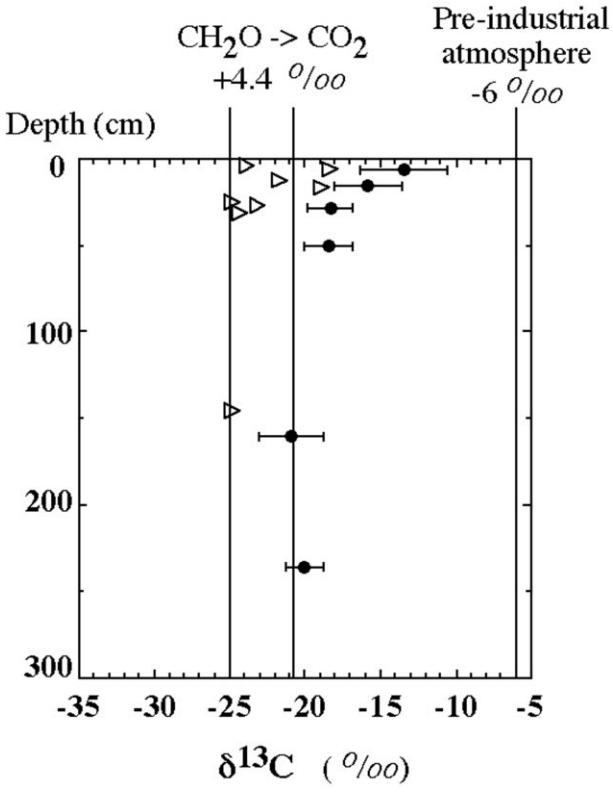

Fig. 5. Whole sample $\delta^{13}C$ (open triangles) and average gibbsite-associated $\delta^{13}C$ values (closed circles) observed in the weathering profile at PMRW ridge-crest site. Horizontal bars represent the range in values observed during individual extractions. Vertical lines (left to right) depict organic matter input, isotopic fractionation expected from CO_2 gas generation and the average pre-industrial atmospheric composition.

parallel galleys of the orthorhombic structure. Fig. 4 shows that the close-packed OH^- and Al^{3+} groups of the gibbsite structure does not offer channel-like sites like goethite. The spaces between the layers are filled with protons. Sites that can potentially harbor $CO_3^{=}$ groups are the vacant charge-deficient octahedral sites and/or along hydroxyl edge defect sites that require excess charge compensation (Hsu, 1989). Carbonate anions that have a strong affinity for Al^{3+} can displace H_2 and OH^- ligands (White and Hen, 1975). Perhaps systematic gibbsite synthesis and spectroscopic studies of reaction products will suggest a mechanism for this process.

5.1. Model for $\delta^{13}C$ distribution in PMRW weathering profile

The distribution and cycling of CO_2 in a weathering profile is clearly a complex phenomenon that involves the interaction of solid, liquid and gaseous phases in a system mediated by short- and long-term tectonic, biological and

climatic variations. It is difficult to envision a model that adequately describes all such interactions. However, the distinct $\delta^{13}C$ trend seen in the CO_2 evolved from the breakdown of gibbsite invites an interpretation in light of existing models for CO_2 produced in soils. Cerling (1984) has provided the most widely used treatment for modeling $\delta^{13}C$ distributions in soils, where it is generally accepted that the unsaturated pore spaces in the subsurface have higher CO_2 partial pressures than does the atmosphere. In the ridge-crest weathering profile site at the PMRW the pores are almost perennially unsaturated in the upper 150 cm. The combined CO_2 production from root respiration and microbial degradation of leaf and wood result in a flux, that over periods of climatic and tectonic stability can be considered steady state.

The equations that describe CO_2 concentration and $\delta^{13}C$ composition of pore space air are thoroughly derived by Cerling (1984). The model is based on steady state one-dimensional Fickian diffusion, where the concentration of pore space CO_2 (C_s, atmos) and its stable carbon isotopic composition (δ_ϕ) are functions of (1) the soil $^{12}CO_2$ and soil $^{13}CO_2$ diffusion coefficients (D_s and D_B, $cm^2\ h^{-1}$), (2) the soil respiration rate or source term for CO_2 (ϕ_s, moles $h^{-1}\ cm^2$), (3) the characteristic depth over which the CO_2 source is producing (L, cm), (4) the depth position in the weathering profile (z, cm), (5) temperature (T, K), (6) the gas constant (R, atmos cm^3 $moles^{-1}$ K^{-1}) and (6) the ‰ value of the respired CO_2 (δ_s) and atmosphere CO_2 (δ_a).

In the modeling results presented below, D_s is treated as a constant, using the 72 $cm^2\ h^{-1}$ value used by Cerling (1984). Values of -24‰ and -6‰ are used for δ_s and δ_a, respectively. The calculated pore CO_2 concentrations as a function of depth in the profile are shown in Fig. 6a. Each curve represents the expected concentrations for soil respiration rates ranging from 0 to 12×10^{-3} moles $h^{-1}\ m^{-2}$. Fig. 6b shows the steady state distribution of $\delta^{13}C$ as a function of depth for the same range of soil respiration rates. Plotted on Fig. 6b are the average $\delta^{13}C$ values of the CO_2 derived from the timed step extractions for the five shallowest samples (6–160 cm).

Comparison between the model curves in Fig. 6b and the isotopic observations has several important implications for the potential to use $\delta^{13}C$ values of CO_2 extracted from gibbsite in the evaluation of atmospheric PCO_2 conditions. Firstly, it appears that the $\delta^{13}C$ signature associated with CO_2 recovered from the thermal breakdown of gibbsite in soils offers a similar opportunity to be a paleoecological indicator as the minerals calcite (Cerling, 1984) and goethite (Yapp, 1996). The coincidence of the observed isotopic trend on the soil respiration line of about 6×10^{-3} moles $h^{-1}\ m^{-3}$ with the average 9×10^{-3} moles $h^{-1}\ m^{-3}$ soil respiration rate for a temperate forest ecosystem at the same latitude as the PMRW (Schlesinger, 1977) suggests that the gibbsite associated $\delta^{13}C$ is directly recording ambient soil CO_2 conditions. Model refinements clearly need to be made. For example, a more accurate assumption for the changes in D_s as a function of depth is needed.

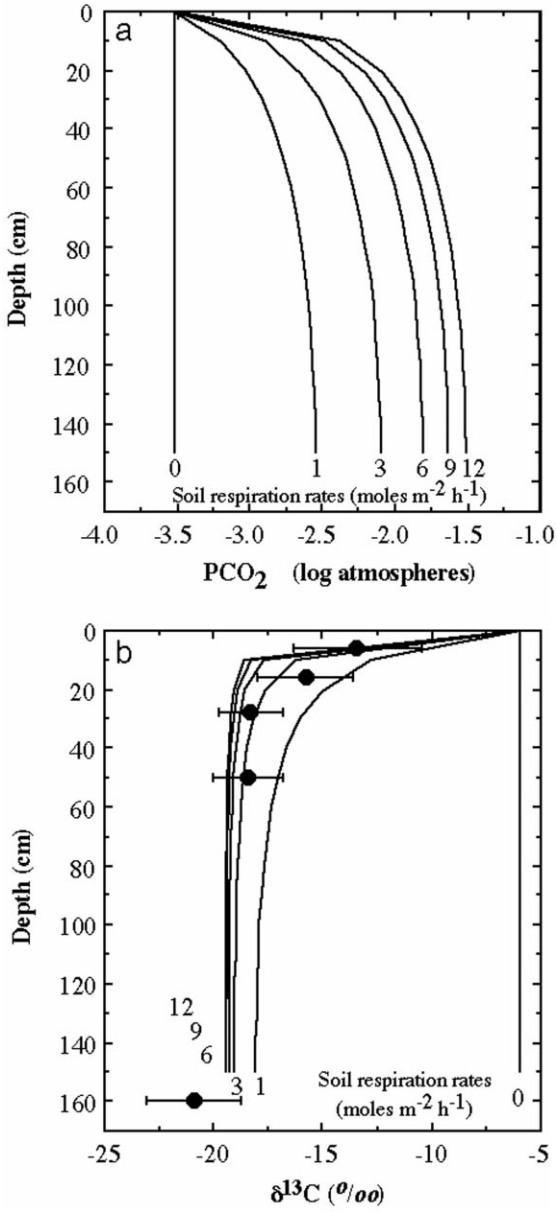

Fig. 6. (a) Pore space gas PCO_2 concentrations predicted from steady-state diffusion model for various soil respiration rates. Note that with zero soil CO_2 production the profile approximates present day concentrations of $\sim$300 ppm. (b) Curves showing the model $\delta^{13}C$ composition of pore space CO_2 assuming different soil respiration rates. See Cerling (1984) and text for model assumptions and boundary conditions. Points plotted on figure are the average observed $\delta^{13}C$ values obtained from the timed-step extractions.

The second implication regards the variations or range in isotopic values measured for each particular extraction in the timed step process. Fig. 2 shows that, depending upon depth, each sample evolves a distinctive pattern of $\delta^{13}C$. Perhaps future high resolution studies of gibbsite (particularly with relatively pure natural gibbsite) and the phase transformations that occur with each timed step will provide insights in to the mechanism for the particular isotopic releases. Given the range of isotopic values observed in this study, if the $\delta^{13}C$ values were applied to a paleo-PCO_2 model such as Yapp (1987) then this would potentially result in a commensurate range of model solutions.

The final implication for the apparent preservation of soil ecological conditions in the gibbsite associated $\delta^{13}C$ record is the potential to monitor changes due to anthropogenic activities. Such changes would include temporal input variations in the $\delta^{13}C$ composition of the organic matter pool, induced either by relative changes in the proportions of biomass produced by plants using C_3 and C_4 photosynthetic pathways or by organic solvent contamination and subsequent microbial respiration. One major limitation is constraining the age of the mineral authigenesis. A suggested method for providing a minimum age is the application of cosmogenic nuclides. Studies are currently underway to determine the ^{10}Be and ^{26}Al derived exposure ages of the same PMRW profile used in this study. Samples are also currently being processed to evolve sufficient quantities of CO_2 from the gibbsite to allow ^{14}C dating.

6. Conclusions

The initial intent of this study was to perform a modern test of the assumptions behind the goethite paleo-PCO_2 barometer proposed by Yapp and Poths (1992). Although goethite is present in the PMRW study site, it occurs only as a minor constituent in the fine fraction. It has been determined that gibbsite is the dominant authigenic metal-hydroxide phase present. Timed-step CO_2 and H_2O extractions at 230 to 240°C, associated with the dehydroxylation phase transformations yield as much as 13 times the amount of CO_2 for the given goethite content (assuming the highest reported $CO_3^{=}$ mole fraction for goethite by Yapp, 1996). It is proposed herein that CO_2 analyzed in this study is a product of carbon sequestered at the time of gibbsite authigenesis. The exact mechanism for sequestration is undocumented at this point in time, but it is suggested that the gibbsite structure can harbor $CO_3^{=}$ groups on vacant charge-deficient octahedral sites and/or along hydroxyl edge defect sites that require excess charge compensation.

The $\delta^{13}C$ composition of the organic matter input to the forest floor at the PMRW is about -25%. The $\delta^{13}C$ associated with gibbsite exhibits a non-linear gradient that asymptotically approaches lighter values of $-21‰$ with depth and $-6‰$ toward the soil–atmosphere interface. This trend coincides with $\delta^{13}C$

values predicted by the model of Cerling (1984) that assumes Fickian diffusive transport of soil gases with boundary conditions defined by $\delta^{13}C$ by the organic matter input, pre-industrial atmospheric conditions and soil respiration rates typical for a temperate forest at the latitude of the PMRW. This modern test of gibbsite and the soil ecological conditions surrounding a temperate forest granitic regolith suggests that gibbsite can be added to the list (that is now comprised of goethite and calcite) of authigenic minerals with the potential to record atmospheric PCO_2 conditions that have existed in the geologic past.

Acknowledgements

This work was supported by a grant to the senior author from the National Science Foundation (EAR9628035). Special thanks go to Doug Crowe and Bill McClain who kindly allowed use of the isotope lab and aided in the construction of the novel extraction line. Donna Shillington and Larry West helped with the DSC work. A special thanks to Crayton Yapp whose insights were innumerable and invaluable.

References

Atkins, R.L., Higgins, M.W., 1980. Superimposed folding and its bearing on geologic history of Atlanta, GA area. In: Frey, R.W. (Ed.), Excursions in Southeastern Geology I Am. Geo. Institute, Atlanta, GA, pp. 19–40.

Balesdent, J., Girardin, C., Mariotti, A., 1993. Site-related $\delta^{13}C$ of tree leaves and soil organic matter in a temperate forest. Ecology 74 (6), 1713–1721.

Berner, R.A., 1994. GEOCARB II: a revised model of atmospheric CO_2 over Phanerozoic time. American Journal of Science 294, 56–91.

Bostick, P.E., 1968. The distribution of some soil fungi on a Georgia granite outcrop. Bull. Ga. Acad. Sci. 26, 149–154.

Bostick, P.E., 1971. Vascular plants of Panola Mountain, Georgia. Castanea 36, 194–209.

Cappellato, R., Carter, M.E.B., 1988. Successional changes in a Piedmont deciduous forest at Panola Mountain State Conservation Park. Association of Southeastern Biologist Bulletin 35, 67, Abstract with programs.

Carter, M.E.B., 1978. A community analysis of the Piedmont deciduous forest of Panola Mountain State Conservation Park, Atlanta, GA. MS Thesis, Emory University, 126 pp.

Cerling, T.E., 1984. The stable isotopic composition of modern soil carbonate and its relationship to climate. Earth and Planetary Science Letters 71, 229–240.

Cerling, T.E., 1991. Carbon dioxide in the atmosphere: evidence from Cenozoic and Mesozoic paleosols. American Journal of Science 291, 377–400.

Cerling, T.E., Quade, J., Wang, Y., Bowman, J.R., 1989. Carbon isotopes in soils and paleosols as ecology and palaeoecology indicators. Nature 341, 138–139.

Craig, H., 1957. Isotopic standards for carbon and oxygen and correction factors for mass spectrometric analysis. Geochimica et Cosmochimica Acta 12, 133–144.

Dixon, J.B., 1989. Kaolin and serpentine group minerals. In: Dixon, J.B., Weed, S.B. (Eds.), Minerals in Soil Environments. 2nd edn. Soil Science Society of America, Madison, WI, pp. 467–526.

Farmer, V.C., 1974. The infrared spectra of minerals, Mineralogical Society.

Holland, W., 1954. The Geology of the Panola Shoals Area: DeKalb County, GA. MS Thesis, Emory University.

Hsieh, J.C.C., Yapp, C.J., 1999. Soil CO_2 budget in a modern weathering profile as inferred from the iron (III) carbonate component in Pedogenic geothite. Geochimica et Cosmochimica Acta, in press.

Hsu, P.H., 1989. Aluminum oxides and oxyhydroxides. In: Dixon, J.B., Weed, S.B. (Eds.), Minerals in Soil Environments. 2nd edn. Soil Science Society of America, Madison, WI, pp. 331–378.

Huntington, T.G., Hooper, R.P., Peters, N.E., Bullen, T.D., Kendall, C., 1993. Water, Energy and Biogeochemical Budgets investigation at Panola Mountain Research Watershed, Stockbridge, GA. U.S. Geological Survey.

Hurst, V.J., 1977. Visual estimation of iron in saprolite. Geological Society of America Bulletin 88, 174–176.

Hurst, V.J., Schroeder, P.A., Styron, R.W., 1997. Accurate quantification of quartz and other phases by powder X-ray diffractometry. Analytica Chimica Acta 337, 233–252.

Kampf, N., Schwertmann, U., 1982. The 5 M NaOH concentration treatment for iron oxides in soils. Clays and Clay Minerals 30, 401–408.

McDonnell, J.J., Freer, J., Hooper, R., Kendall, C., Burns, D., Beven, K., Peters, J., 1996. Temporal and spatial variability of soil water potential at the hillslope scale. EOS, Transactions of the American Geophysical Union, 77 (47), 465, 470.

Megaw, H.D., 1934. The crystal structure of hydroargillite $Al(OH)_3$. Z. Kristallogr. 87, 185–204.

Melear, N.D., 1990. Clay Minerals and Ferruginous Minerals Formed During Weathering of Granitic Rocks of the Georgia Piedmont. MS, Department of Geology Athens, University of Georgia. 69 pp.

Melear, N.D., 1998. Crystal Properties of Goethite and Hematite from three Weathering Profiles of the Georgia Piedmont, PhD Department of Geology: Athens, University of Georgia.

Melear, N.D., Schroeder, P.A., 1998. Crystal chemistry of goethites from selected weathering profiles of the Georgia Piedmont: evidence for multigenerational mineral assemblages. Geoderma, in review.

Nixon, R.A., 1981. Rates and Mechanisms of Chemical Weathering in an Organic Environment at Panola Mountain, Georgia, PhD Thesis Emory University; Atlanta, GA, 182 pp.

Quade, J., Cerling, T.E., Bowman, J.R., 1989. Systematic variations in the carbon and oxygen isotopic composition of pedogenic carbonate along elevation transects in the southern Great Basin, United States. G.S.A. Bulletin 101, 464–475.

Ragsdale, H.L., Harwell, M.A., 1969. A map of the island ecosystems of Panola Mountain. Bull. Ga. Acad. Sci. 27, 83.

Schlesinger, W.H., 1977. Carbon balance in terrestrial detritus. Ann. Rev. Ecol. Syst. 8, 51–81.

Schroeder, P.A., Pruett, R., 1996. Iron ordering in kaolinites: insights from ^{29}Si and ^{27}Al NMR spectroscopy. American Mineralogist 81, 26–38.

Schroeder, P.A., Pruett, R.J., Hurst, V.J., 1998. Effects of secondary iron phases on kaolinite ^{27}Al MAS NMR spectra. Clays and Clay Minerals 46 (4), 429–435.

Singh, J.S., Gupta, S.R., 1977. Plant decomposition and soil respiration in terrestrial ecosystems. Botanical Review 43 (4), 449–528.

Tissot, B.P., Welte, D.H., 1978. Petroleum Formation and Occurrence: A New Approach to Oil and Gas Explorations. Spinger-Verlag.

Violante, A., Gianfreda, L., Violante, P., 1993. Effect of prolonged aging on the transformation of

short-range ordered aluminum precipitation products formed in the presence of organic and inorganic ligands. Clays and Clay Minerals 41 (3), 359–535.

White, J.L., Hen, S.L., 1975. Role of carbonate in aluminum hydroxide gel established by Raman and IR analysis. J. Pharm. Sci. 64, 264–265.

White, A.F., Bullen, T.D., Vivit Davison, V., Schulz, M.S., 1997. The role of trace disseminated calcite in the weathering of granitoid rocks. Geological Society of America Annual Meeting, Salt Lake City, UT. Abstract No. 50317.

Yapp, C.J., 1987. A possible goethite–iron (III) carbonate solid solution and the determination of CO_2 partial pressures in low temperature geologic systems. Chemical Geology 64, 259–268.

Yapp, C.J., 1991. Oxygen isotope in an oolitic ironstone and the determination of goethite $\delta^{18}O$ values by selective dissolution of impurities: the 5 M NaOH method. Geochimica et Cosmochimica Acta 55, 2634–2677.

Yapp, C.J., 1996. The abundance of $Fe(CO_3)OH$ in goethite and a possible constraint on minimum atmospheric oxygen partial pressures in the Phanerozoic. Geochimica et Cosmochimica Acta 60 (22), 4397–4402.

Yapp, C.J., Poths, H., 1986. Carbon in natural goethites. Geochimica et Cosmochimica Acta 50, 1213–1220.

Yapp, C.J., Poths, H., 1990. Infrared spectral evidence for a minor Fe(III) carbonate-bearing component in natural goethite. Clays and Clay Minerals 38, 442–444.

Yapp, C.J., Poths, H., 1991. $^{13}C/^{12}C$ ratios of the Fe(III) carbonate component in natural goethite. In: Taylor, H.P., O'Neil, J.R., Kaplan, I.R. (Eds.), Stable Isotope Geochemistry: A Tribute to Samual Epstein. The Geochemical Society, pp. 257–270, Special Publication No. 3.

Yapp, C.J., Poths, H., 1992. Ancient atmosphere CO_2 pressure inferred from natural goethites. Nature 355, 342–344.

Yapp, C.J., Poths, H., 1993. The carbon isotope geochemistry of goethite (α-FeOOH) in the Upper Ordovician Neda Formation ironstone: implications for early Paleozoic continental environments. Geochimica et Cosmochimica Acta 57, 2599–2611.

Yapp, C.J., Poths, H., 1994. Productivity of pre-vascular continental biota inferred from the $Fe(CO_3)OH$ content of goethite. Nature 368, 49–51.